Astron. Astrophys. 158, 119–134 (1986)

ASTRONOMY
AND
ASTROPHYSICS

# Time-dependent chemistry in dense molecular clouds

## II. Ultraviolet photoprocessing and infrared spectroscopy of grain mantles

**L.B. d'Hendecourt[1,2], L.J. Allamandola[1,3], R.J.A. Grim[1], and J.M. Greenberg[1]**

[1] Laboratory Astrophysics, Huygens Laboratorium, Wassenaarseweg 78, NL-2300 RA Leiden, The Netherlands
[2] Groupe de Physique des Solides de l'E.N.S., T23, 4 Place Jussieu, F-75251 Paris Cedex 05, France
[3] NRC Senior Research Associate, NASA Ames Research Center, Mail Stop 245/6, Moffett Field CA 94035, USA

Received May 17, accepted September 16, 1985

**Summary.** We have performed a series of experiments in which mixtures of gases condensed on a substrate at 10 K are irradiated with ultraviolet light in order to probe the photochemical processing of interstellar ices. The evolution of these simulated grain mantles is followed by infrared spectroscopy (2.5–20 $\mu$m). Upon photolysis, the appearance of new bands in the spectra is observed and their possible identification is discussed. Rough quantitative estimates of the photo-production rate of new molecules are given and some infrared cross sections of a few of these bands are discussed. The main results show that:

*i*) $CO_2$ and $H_2CO$ should be formed abundantly on grains via this process and their high production rate should influence the gas phase as well.

*ii*) the similarities between the infrared spectra of processed ices and the spectrum of W 33 A show that the energetic processes modifying the composition of the icy mantles in most regions of dense clouds are very efficient.

*iii*) infrared cross sections of a few bands observed in our spectra and in the spectrum of W 33 A are given, using conservative estimates of the number of molecules in the laboratory samples. These cross sections suggest that the species giving rise to the "6.8 $\mu$m" band are limited to a class of molecules in which the —$CH_2$ —and —$CH_3$ groups are adjacent to unsaturated groups as found in ketones, esters and alcohols.

Finally, the importance of laboratory work coupled with infrared astronomy in furthering our understanding of the composition of interstellar ices, is stressed.

**Key words:** infrared radiation – interstellar medium: clouds – dust – molecules –

### 1. Introduction

In a previous paper, d'Hendecourt et al. (1985, hereafter Paper I) calculate the time dependent behavior of the composition, abundance and distribution of molecules in both the gas and solid phases in dense molecular clouds, using a method that takes atomic and molecular processes simultaneously into account. In view of the fact that results of models considering only gas phase chemistry and their comparison with observations have been the subject of considerable discussion in the literature and that the influence solid state chemistry and physical processes have on the gas phase composition was extensively discussed in Paper I, we focus here on the effects energetic processing has on the solid state.

Infrared spectroscopy is a powerful tool for the study of molecular grain mantles in dense interstellar clouds (see eg. Allamandola, 1984). For this purpose, and somewhat arbitrarily, the infrared region can be separated into two distinct regions: the mid infrared ($2 \leqq \lambda \leqq 20\,\mu$m) and the far infrared ($\lambda \geqq 20\,\mu$m). The first region contains the characteristic frequencies of molecular vibrations and, in favorable cases, allows one to identify a given molecule directly. However, due mainly to overlapping of bands and observational limitations, band assignment is generally limited to a molecular subgroup. The spectral profile of the features observed in interstellar objects show that, in some cases, the molecules responsible for these features are adsorbed on interstellar grains (Soifer et al., 1979; Aitken, 1981; Willner et al., 1982; Knacke et al., 1982). Such accretion mantles can be simulated and studied in the laboratory in a straightforward way by condensing gases either as pure substances or as mixtures of different cosmically abundant molecules onto a cold (10 K) surface and measuring the infrared absorption spectrum of these ices. The comparison of such laboratory spectra with interstellar spectra has led first to the identification of water in the amorphous ice form (Léger et al., 1979) being largely responsible for the peculiar shape of the strong 3 $\mu$m absorption band, long thought to be due to water ice, but with an unusual profile. Peak to peak comparison between laboratory spectra and spectra from compact infrared sources over the entire mid-infrared spectral range has proven to be invaluable, not only for the identification of other constituents (Hagen et al., 1980), but also as a probe of the chemistry taking place on the surface or in the bulk of the grains (Tielens et al., 1984).

At the present time, prominent absorption features at 2.97, 3.07, 3.4, 4.61, 4.67, 6.0 and 6.8 $\mu$m have been observed which are attributed to mantle constituents (see Allamandola, 1984 and references therein for a review). The bands are mostly associated with protostellar objects because these objects consist of powerful infrared sources embedded in dense molecular clouds. The strongest bands (2.97, 3.07, 4.61, 6.0 and 6.8 $\mu$m) are primarily attributed to the simplest molecules expected to be the most

*Send offprint requests to:* L.B. d'Hendecourt

abundant on grains e.g. $H_2O$, $NH_3$ and CO, with the 6.8 $\mu$m band attributed to the $-CH_3$ group, probably part of a somewhat larger molecule (Hagen et al., 1980). Unfortunately, some interesting and presumably abundant molecules (e.g. $O_2$, $N_2$) cannot be measured in the infrared. Others such as CO and $CH_4$, which possess somewhat narrower bands in the solid state, are extremely difficult to detect because they lie in a region of the spectrum which is heavily attenuated by the earth's atmosphere and require good signal-to-noise data at a resolution higher than is currently available. Nevertheless, the model calculations described in Paper I as well as similar calculations of Tielens and Hagen (1982) predict that these molecules should be produced efficiently on grains and remain as mantle constituents. Thus, laboratory spectra of these mixtures should be studied and compared with observations to test these predictions. Furthermore, and perhaps more compelling for such studies, is the fact that the features near 3.4 $\mu$m (Allen and Wickramasinghe, 1981), 4.67 $\mu$m (Lacy et al., 1984) and part of the 6.8 $\mu$m band (Tielens et al., 1984) cannot be explained by mixtures containing these simple molecules alone but imply a much richer chemistry, involving hydrocarbons more complex than $CH_4$ and molecules containing the cyano group, CN. Presumably, these features originate in molecules which are produced by more energetic chemical processes such as ultraviolet photolysis or cosmic-ray bombardment. The wide variety of molecular reactions made possible by high energy processes cannot be taken into account in a computer simulation model, since the number of reactants and reaction channels increases considerably if reactions having an appreciable activation energy are allowed to proceed in the bulk of the grain mantle (see Paper I). Fortunately, this more complicated chemistry can also be simulated in reasonably straightforward laboratory experiments where the ices are irradiated with ultraviolet light and the photochemical evolution of these "mantles" is followed by infrared spectroscopy.

In this paper, we describe the experiments performed in the laboratory to understand the extent to which a given mantle composition can be modified by ultraviolet irradiation and determine the influence this process has on grain mantle evolution in dense clouds. The results of these experiments are intimately connected to the results given in Paper I. A short description of the experimental techniques used is presented in Sect. 2 and in Sect. 3, mantle compositions which have been calculated under various conditions are reviewed and the corresponding infrared spectra (2.5–20 $\mu$m) are briefly discussed. Section 4 presents the various modifications of the spectra and composition of the mixtures brought about by ultraviolet radiation. Quantitative estimates of molecules production/destruction rates are tentatively given. Integrated intensities of the various bands relevant for the interpretation of astronomical spectra are also estimated and are used to identify some of the new molecules and molecular sub-groups formed upon irradiation. An attempt is made to discuss the extent to which time evolution of the interstellar mantles can be deduced from the data by scaling our laboratory results to plausible interstellar cases. New mantle compositions are given which constitute a "second order" correction to the initial composition calculated in Paper I which only includes simple grain surface low temperature reactions into account. In Sect. 5 the main astrophysical implications are discussed, briefly for the gas and more extensively for the solid phase by applying the results derived in Sect. 4 to the interpretation of the infrared spectrum of the protostellar object W 33 A. We conclude by discussing the overall importance and validity of these processes and review which regions of the infrared spectrum opened up by space born instruments should be observed in the future in order to gain more insight in the molecular composition of the solid phase of dense clouds and the role this plays in the chemistry.

## 2. Experimental techniques

The main points of the experimental set up are briefly reviewed here; details can be found in Hagen et al. (1979). Mixtures containing simple molecules in various ratios (see Sect. 3) are prepared in a greaseless glass vacuum system. After allowing sufficient time for thorough mixing, the gas is slowly deposited (10 micron/hour) onto a cold (10 K) CsI window for infrared transmission studies. Typical deposition times ranged from 1–5 minutes. The sample substrate is mounted in a metal vacuum chamber evacuated to a pressure of $2\,10^{-7}$ mbar by a turbo-molecular-rotary pump combination. The substrate can be kept cold for an indefinite amount of time by a closed-cycle helium refrigerator. Sample thickness is measured by monitoring He/Ne laser interference fringes reflected off the sample. The samples are photolyzed during a fixed amount of time with a microwave excited hydrogen lamp providing a calibrated ultraviolet photon flux. Infrared spectra are taken after deposition, before and after irradiation and after warmup. All infrared spectra analyzed quantitatively were measured in transmission with 2 $cm^{-1}$ resolution ($\Delta\lambda/\lambda = 2\,10^{-4}$ at 4 $\mu$m) from 4000 to 500 $cm^{-1}$ (2.5 to 20 $\mu$m) by a Digilab FTS-15 Fourier Transform Infrared Spectrometer. By measuring the total integrated absorbance values over different bands from these spectra, the total number of molecules in the sample can be obtained, provided the integrated absorbance, $A$, of a given molecule is known. Although large uncertainties might be expected from these absolute measurements in solids, for some bands it is possible to follow the evolution of the sample during photolysis quantitatively, thus providing insight into the main reaction channels and deriving a mean production rate for a given molecule. Integrated intensities of infrared bands of a number of molecules in the solid phase at 10 K have been carefully measured in the laboratory (d'Hendecourt and Allamandola, 1986, Paper III) and are used in this paper as calibrated standards for quantitative studies.

Sample thicknesses are small (0.2–0.5 $\mu$m): the samples are optically thin to the ultraviolet radiation so that the scaling of the laboratory production rates of new molecules to interstellar clouds production rates is meaningful. Photolysis is made only after deposition of the sample when it has a true temperature of 10 K.

## 3. Experimental 'mantle' composition

One difficulty inherent in carrying out such laboratory experiments is the choice of the mixtures to be studied. Although some arguments in favor of a composition containing the different elements in a ratio in agreement with cosmic abundances seem reasonable, the observed gas phase abundances of molecules in interstellar clouds show that, apart from $H_2$, CO is the most abundant molecule whereas, for the solid phase, the 3.1 $\mu$m band suggests that $H_2O$ dominates. Thus, choosing the initial mixture based on observations alone is rather uncertain. We adopt the approach that theoretical modelling which includes gas as well as solid state processes such as that of Tielens and Hagen (1982)

**Table 1.** Mantle composition at $10^8$ years, obtained, as described in Paper I, for the various cloud parameters. The numbers are listed separately

| | $A_v = 2$ $n_0 = 10^3$ | $A_v = 4$ $n_0 = 10^4$ | $A_v = 8$ $n_0 = 10^5$ |
|---|---|---|---|
| $H_2O$ | 62 | 50 | 3 |
| CO | 18 | 3 | 30 |
| $CH_4$ | 4 | <1 | 0.4 |
| $NH_3$ | 9 | <1 | 0.4 |
| $O_2$ | — | 3 | 43 |
| $N_2$ | — | 7 | 8 |
| $CO_2$ | 2[a] | 32[a] | 9[a] |

[a] The surface reaction $CO + O \rightarrow CO_2$ has been taken into account for the computation of this table. If this is not the case the amount of $CO_2$ is reduced to about 1% for the standard case ($A_v = 4$, $n_0 = 2\,10^4\,cm^{-3}$) and the abundance of CO goes up to ≃31% (see Grim and d'Hendecourt, 1986, Paper IV)

or our work (Paper I) provides the insight needed to select the initial mixtures.

Composition depends not only on cloud age, but also on various conditions such as initial elemental abundance and visual extinction to a particular point in a cloud. To understand the choice of the particular mixtures used, we briefly review the main results of that work. Mantle compositions are listed in Table 1, calculated as a function of various cloud parameters for an age of $10^8$ years. While there are obvious differences between each composition, they can be grouped into two classes: those in which $H_2O$ is dominant; and those in which CO and $O_2$ are dominant with $H_2O$ representing only about 3% of the mixture. The initial elemental abundances assumed for these calculations are taken from Morton (1974) for the ξ Oph molecular cloud where the O/C ratio is large, around 3.2. In our model, as in the majority of models describing gas phase chemistry using an ion molecule reaction scheme (eg. Prasad and Huntress, 1978; Graedel et al., 1982), carbon is efficiently converted to the stable CO molecule in about $10^6$ years. As a result, less stable carbon bearing species such as $CH_4$ have a tendency to gradually disappear from the mantle as the C gets bound up in CO. Thus, although methane is made efficiently on the grains at short times, it is not abundant at longer times because the permanent cycling of the molecules between the solid and the gas phases progressively transforms the carbon contained in the $CH_4$ to CO (see Paper I). In a similar way, nitrogen is also converted to $N_2$ at long times but ammonia remains more abundant than $CH_4$. For low and intermediate values of extinction ($A_V \leqq 4$), water always dominates because, in the gas phase, oxygen remains atomic and atomic hydrogen is more abundant than oxygen. The production of $H_2O$ on grain surfaces is thus always effective. For higher extinction, the oxygen extinction and density. For extreme cases ($A_V \sim 10$, not described in the paper), water represents a minor constituent of the mantle (about 2%), the rest being mainly $O_2$ and CO. The two following mixtures were chosen to represent the two distinct classes: Mixture 1: $H_2O/CO/CH_4/NH_3$, 6/2/1/1 and Mixture 2: $H_2O/CO/O_2/CH_4/NH_3/N_2$, 1/1/1/0.3/0.3/0.03. Mixture 1 corresponds to our standard case at equilibrium ($n_0 = 2\,10^4$, $A_V = 4$), reached in about $3\,10^6$ years and Mixture 2 to a higher extinction case ($n_0 = 10^5$, $A_V = 8$) in the course of its evolution ($3\,10^7$ years). In this case, complete equilibrium is not reached until about $5\,10^7$ years. Carbon dioxide, an important constituent of the standard model has not been included here with the amount of $CO_2$ replaced by the corresponding amount of CO. The occurrence of the major $CO_2$ production reaction used ($CO + O \rightarrow CO_2$) on the low temperature surface of the grain is in fact highly questionable as shown by a laboratory study of this reaction (d'Hendecourt, 1984; Grim and d'Hendecourt, 1986). Therefore the $CO_2$ abundance predicted in the standard case calculation is probably an overestimate. It should be noted that all the calculated mixtures consist of quite simple molecules, e.g. even formaldehyde is not abundant (<1%). This is largely determined by the limitations placed on the reaction pathways, inherent in low temperature surface reactions in general and partly due to the limited grain chemistry used in the program. Finally, because of the complexity of the chemistry initiated by the UV irradiation of these multicomponent mixtures, in analyzing our data we have relied heavily on results of many similar experiments not discussed here as well as those of Hagen (1982) and Van de Bult (1986).

## 4. Mantle modification by UV photoprocessing

### *4.1. Infrared spectra of unirradiated ices*

The spectra of the initial and irradiated mixtures (Mixtures 1 and 2) are displayed in Figs. 1 and 2 for direct comparison, with the initial mixture spectra shown in the upper frames and their irradiated counterparts in the lower frames. Fig. 1 represents the water rich mixture and Fig. 2 the $CO/O_2$ rich case. The exact composition of each mixture is indicated in the figure. Since these spectra of the non-photolyzed mixtures have already been discussed in Paper I, only a brief summary is included here.

In Mixture 1, water ice is largely responsible for the prominent absorption feature at 3.08 μm. The depth of this band is extremely large due to hydrogen bonding between the water molecules (Van Thiel et al., 1957), increasing in strength by a factor of about 25 in going from the gas to the amorphous solid phase (Hagen et al., 1981). Although in this mixture $H_2O$ represents up to 60% of the sample, water molecules with free OH groups are still present as shown by the band located at $3650\,cm^{-1}$ (2.74 μm). This region is an extremely important indicator of the degree of mixing or isolation of water molecules in a given mantle. The OH bending mode absorbs at $1640\,cm^{-1}$ (6.1 μm), and, as described by Hagen et al. (1981), is much less sensitive to hydrogen bonding or interactions with other ice constituents. The other absorption band characteristic of water in molecular ices, a strong and broad absorption which shifts from 820 in pure $H_2O$ for $725\,cm^{-1}$ in molecular ices (13.8 μm), is due to the librational motion (hindered rotation) of the water molecule (Hagen et al. 1981). This band is always present in our spectra, even when water is more diluted (Mixture 2).

The CH-stretch of methane is observed at $3010\,cm^{-1}$ (3.32 μm), on the shoulder of the ice band and is broadened compared to pure methane. The bending mode of $CH_4$ produces a sharp absorption at $1305\,cm^{-1}$ (7.7 μm). Carbon monoxide has a single absorption at $2143\,cm^{-1}$ (4.67 μm) with the weak line at $2090\,cm^{-1}$ (4.78 μm) due to the $^{13}CO$ isotope. We note here that the ratio of the integrated intensities of these two lines is about 1/90, corresponding to the natural $^{13}C/^{12}C$ isotopic ratio, a value

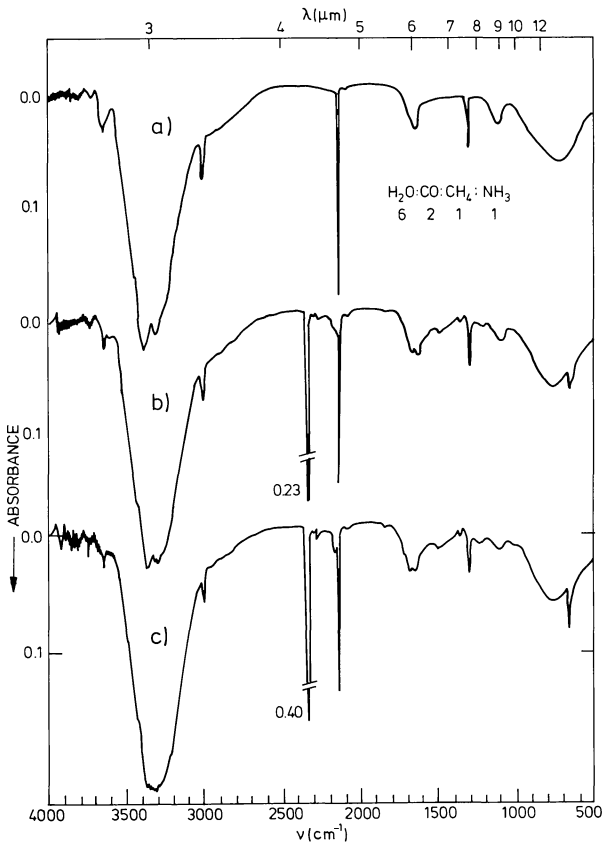


**Fig. 1a–c.** Infrared spectra of Mixture 1: (**a**) No irradiation, (**b**) and (**c**) After 4 and 24 hours of irradiation respectively. See Table 3 for the number of molecules corresponding to the absorbances

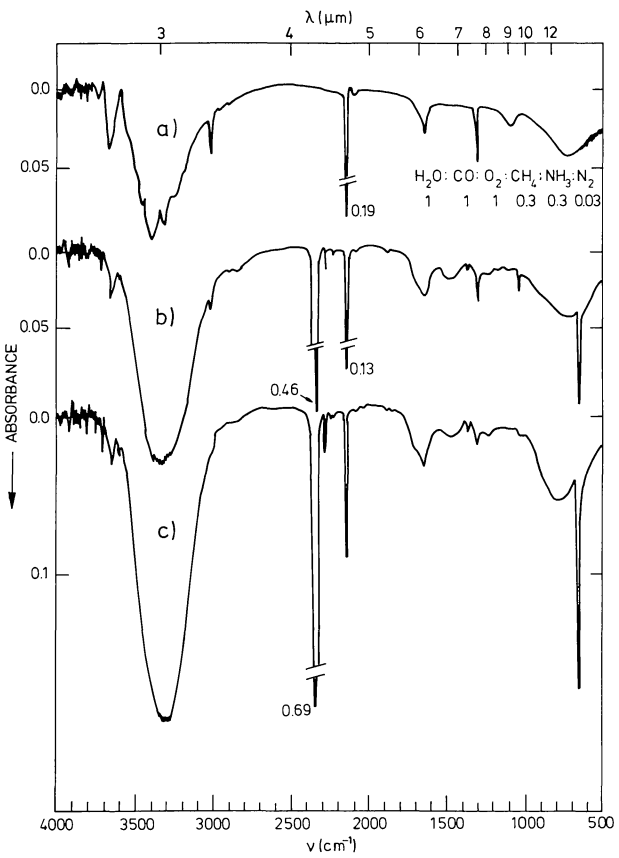


**Fig. 2a–c.** Infrared spectra of Mixture 2: (**a**) No irradiation (**b**) and (**c**) After 4 and 24 hours of irradiation respectively. See Table 3 for the number of molecules corresponding to the absorbances

which makes us confident of the number of CO molecules derived from the band strength whether initially present and (or) appearing in the sample upon irradiation. Ammonia has three absorption bands: 3380 $cm^{-1}$ (2.96 $\mu$m), 1630 $cm^{-1}$ (6.13 $\mu$m) and about 1100 $cm^{-1}$ (9.1 $\mu$m), this latter band is particularly characteristic of solid ammonia and used for quantitative studies. In this mixture ammonia also produces the long wavelength wing on the 3.1 micron ice band; however other strong bases can produce this as well (Hagen et al., 1980, 1983a,b). The wing makes the observation of weaker bands in this region of the spectrum extremely difficult; especially effected is the search of the CH-stretch in saturated hydrocarbons (Allamandola, 1984; Tielens et al., 1984).

Mixture 2 differs primarily in the 3 micron region where, due to the relatively low concentration of water (26%) in the sample, some water molecules can be found isolated, giving rise to the strong absorption at 3650 $cm^{-1}$ while the resulting 3.1 $\mu$m ice band is markedly different from the previous case. The two other important water features around 6 and 13 micron are present, showing clearly that neither the absolute or relative intensity of these two bands depends significantly upon the degree of isolation. The other bands due to $CH_4$, CO and $NH_3$ are not markedly mixture dependent.

### *4.2. Infrared spectra of irradiated ices*

Irradiation produces several changes and the resulting spectra differ, not only from those of the initial mixtures but also with respect to each other: new bands appear and many changes can be observed throughout the spectra. First, the qualitative changes will be discussed, focusing on the identification of the new molecules produced which give rise to these new bands, followed by a discussion of the similarities and differences between the spectra associated with the mixtures and the features observed in astronomical objects. Uncertainties in the infrared integrated absorption coefficients of molecules imbedded in mixtures coupled with the difficulties associated in the determination of the correct baseline make quantitative studies of all the bands rather difficult.

The photolyzed mixture spectra shown in Fig. 1b, c and 2b, c have been taken after 4 and 24 hours of irradiation respectively. Apart from allowing the identification of new molecules and radicals formed, these spectra can also be used to extract timescales for the evolution of interstellar mantles. Since the ultraviolet photon flux is known in the laboratory, the photochemical production rate of the new most abundant molecules formed, as well as a photodestruction rate of the parent molecules, can be derived.

#### 4.2.1. Mixture 1 evolution ($H_2O$:CO:$CH_4$:$NH_3$ = 6/2/1/1)

The bands characterising methane, ammonia and, to a lesser extent, carbon monoxide, steadily decrease due to photolysis and subsequent reaction. Photodissociation thresholds and absorptivities at 1600 Å for the molecules of interest are given in Table 2. To a first approximation, CO is not readily photodissociated whereas $CH_4$ and $NH_3$ are. However, absorption

**Table 2.** Photodissociation thresholds, absorptivities at 1600 Å and primary photoproducts of molecules present in the samples (from Hagen, 1982)

| | | $\lambda$ [Å] | $k$ at 1600 Å [$atm^{-1}\,cm^{-1}$, base e] | Primary products |
|---|---|---|---|---|
| Gas | CO | 1118 | 0.3 | |
| | $H_2O$ | 2420 | 100 | H + OH |
| | $H_2$ | 2767 | 0 | |
| | $O_2$ | 2424 | 115 | $O(^3P) + O(^1D)$ |
| | $CO_2$ | 2275 | 4 | $CO + O(^1D)$ |
| | $H_2CO$ | 3483 | <10 | $H + HCO, H_2 + CO, 2H + CO$ |
| | $NH_3$ | 2820 | 10 | $NH_2 + H$ |
| | $N_2$ | 1270 | <0.1 | |
| | $CH_4$ | 2770 | 0.03 | $CH_3 + H$ |
| Solid | $H_2O$[a] | | 470 | |
| | $NH_3$[b] | | 1600 | |
| | $CH_4$[b] | | <3 | |

[a] Van Hemert, 1981
[b] Dressler and Schnepp, 1960; all other data from Okabe (1978)

into the forbidden Cameron band system of CO produces metastable excited state CO molecules which can react with other species in the mixture. For example, photolysis of gaseous CO produces $C_2$ (Hack and Langel, 1981). Water can also be efficiently dissociated. However, as is clear from Fig. 1, presumably due to the high content (60%) of $H_2O$ in the sample, the majority of the $H_2O$ photodissociation products recombine again so that the net photodissociation rate of this molecule is small.

The most intense new bands appear at 2343 $cm^{-1}$ (4.27 $\mu$m; FWHM = 12 $cm^{-1}$), 2167 $cm^{-1}$ (4.61 $\mu$m; FWHM = 25 $cm^{-1}$, width difficult to estimate), 1850 $cm^{-1}$ (5.41 $\mu$m; FWHM = 15 $cm^{-1}$), 1470 $cm^{-1}$ (6.8 $\mu$m; FWHM = 100 $cm^{-1}$), 1370 $cm^{-1}$ (7.3 $\mu$m; FWHM = 20 $cm^{-1}$), 1220 $cm^{-1}$ (8.2 $\mu$m; FWHM = 50 $cm^{-1}$) and finally 660 $cm^{-1}$ (15.2 $\mu$m; FWHM = 22 $cm^{-1}$). Weaker bands are observed around 2960 $cm^{-1}$ (3.38 $\mu$m), 2900 $cm^{-1}$ (3.45 $\mu$m), 2830 $cm^{-1}$ (3.53 $\mu$m), 1090 $cm^{-1}$ (9.2 $\mu$m; FWHM = 15 $cm^{-1}$) and 1020 $cm^{-1}$ (9.8 $\mu$m; FWHM = 20 $cm^{-1}$). The region 1800–1400 $cm^{-1}$ shows many changes which have to be discussed separately because of the complexity of the spectra and blending between lines. Spectra from 2000 to 1000 $cm^{-1}$ (5–10 $\mu$m), taken before and after photolysis are shown on an expanded scale in Fig. 3. Other absorptions which appear in this region are: 1720 $cm^{-1}$ (5.81 $\mu$m), 1695 $cm^{-1}$ (5.90 $\mu$m, a very strong and very broad absorption, FWHM = 45 $cm^{-1}$), and 1585 $cm^{-1}$ (6.31 $\mu$m, a weak, broad and very shallow absorption). To improve the lower signal to noise ratio inherent in the transmission spectra of this sample required to make quantitative estimates of band strength, similar experiments, using the same mixtures, have been performed in reflection where the signal to noise ratio of the data is high enough to confirm the presence of the weakest lines, namely those in the 3000–2800 $cm^{-1}$ region. The presence of some of the weakest and most severely blended bands has been tested by difference spectroscopy and illustration is given in Sect. 4.2.3 below. Note that the absorption due to water ice, around 1610 $cm^{-1}$, does not change much upon photolysis.

The ratio and position of the strongest new lines, those at 2347 $cm^{-1}$ (4.26 $\mu$m) and 660 $cm^{-1}$ (15.2 $\mu$m), allow the unequivocal identification of the $CO_2$ molecule. These lines correspond respectively to the $\nu_3$ (antisymmetric stretching) and to the $\nu_2$ (bending) modes of the $CO_2$ molecule (Shimanouchi, 1972). The absorbance of the antisymmetric stretching mode of carbon dioxide is extremely strong, about one order of magnitude greater than that of the bending mode of $CO_2$ and stretching mode of carbon monoxide (Gribov and Smirnov, 1962). Due to this it is possible to observe the $^{13}CO_2$ isotope which absorbs at 2290 $cm^{-1}$ (4.37 $\mu$m).

The next molecule which can be readily assigned with confidence is formaldehyde ($H_2CO$), with the lines at 1720 and 1500 $cm^{-1}$ (5.8 and 6.69 $\mu$m) corresponding to the CO-stretch

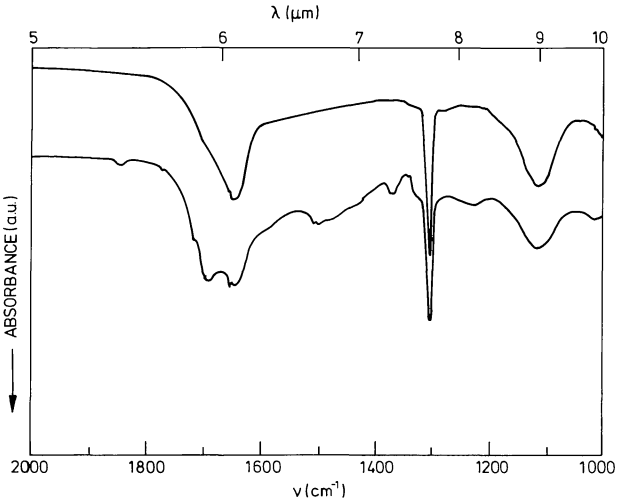


**Fig. 3.** Infrared spectra between 2000 and 1000 $cm^{-1}$ of Mixture 1, $H_2O/CO/CH_4/NH_3$ (6/2/1/1) before (*top*) and after 4 hours of irradiation (*bottom*). Note the apparent deformation of the 6.0 $\mu$m solid $H_2O$ band due to blending with new absorptions while its depth does not increase significantly (both spectra are displayed on the same scale)

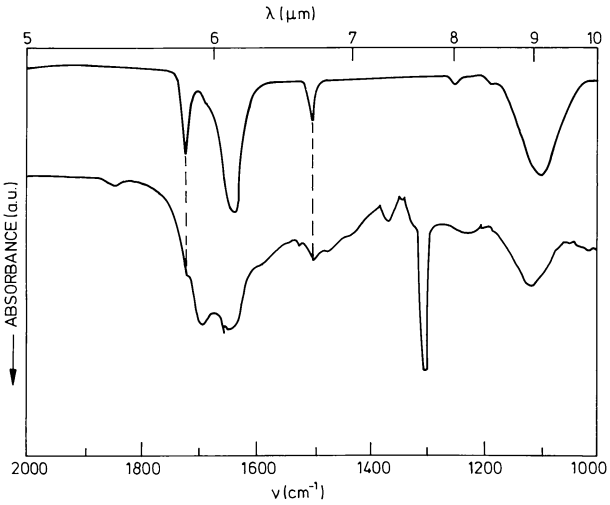


**Fig. 4.** Comparison between the infrared spectra from 2000 to 1000 $cm^{-1}$ (5 to 10 $\mu m$) of a mixture containing $H_2CO$ (*top*) with that of Mixture 1 irradiated for 4 hr (*bottom*) and showing the presence of $H_2CO$. The $H_2CO$ containing mixture is $H_2CO/NH_3/H_2O/CO_2CO(1/1/3/5/10)$ at 10 K. The bands connected by dotted lines are due to $H_2CO$ while the 1640 and 1100 $cm^{-1}$ bands in the upper spectrum are due to $H_2O$ and $NH_3$ respectively

and the $CH_2$ scissoring modes respectively (Schimanouchi, 1972; Van der Zwet et al., 1985). Although this region of the spectrum is difficult to interpret because of overlap with the 6 $\mu m$ water and ammonia bands, the identification of $H_2CO$ is established by comparison of this and other spectra with the spectrum of $H_2CO$ suspended in an ice made up of $H_2O$, $NH_3$, $CO_2$ and CO taken by Van der Zwet et al. (1985), see Fig. 4. The two $H_2CO$ lines at 1720 and 1500 $cm^{-1}$ match the ones obtained in our spectrum in position and roughly in intensity. Formaldehyde also gives rise to the two weak lines at 2830 and 2895 $cm^{-1}$ evident in Figs. 1b and 1c, corresponding to the symmetric and antisymmetric CH stretching vibrations. This identification of $H_2CO$ is further supported by the presence of absorptions at 1850 $cm^{-1}$ and 1090 $cm^{-1}$ (weak) due to the HCO radical (Milligan and Jacox, 1964, 1971), the intermediate in $H_2CO$ production. Photodissociation of $H_2O$, $CH_4$ or $NH_3$ is expected to produce the formyl radical via the reaction $H + CO \rightarrow HCO$ which can then further react with other hot hydrogen atoms, produced by the photodissociation of other molecules, to form $H_2CO$. The much weaker and broader 2490 $cm^{-1}$ band of HCO was not detected in our spectra.

In addition to the new bands attributable to the specific molecules $CO_2$ and $H_2CO$, others appear which, while not assignable to a specific molecule, do indicate the presence of particular molecular subgroups. These will now be discussed in turn.

*i) 2167 $cm^{-1}$ (4.61 $\mu m$).* This band, adjacent to the CO absorption band at 2143 $cm^{-1}$, grows steadily upon irradiation at 10 K. Although the precise identification of this band is not possible on the basis of these experiments alone, the recent observation of a similar band in the spectrum of the protostellar object W 33 A (Lacy et al., 1984) makes a discussion of it, both in terms of identification and importance in grain mantle evolution, quite relevant. This absorption only appears in mixtures containing nitrogen and carbon and is close to the frequency range expected for cyano group (C≡N) stretching vibrations (Bellamy, 1956; Socrates, 1981). However, in a normal cyano containing substance, such as acetonitrile, $CH_3CN$, the CN stretching vibration is at 2265 $cm^{-1}$ (Kitson and Griffith, 1956), 100 $cm^{-1}$ shifted from the observed line. Although shifts can be expected in the solid environment, the spectrum of acetonitrile diluted in a water matrix does not show such a large shift (Paper III). Frequency shifts of the cyano absorption can also occur when an electron rich substituent is attached to the common carbon atom. This can lower the frequency of the cyano absorption by as much as 25 $cm^{-1}$ (Kitson and Griffith, 1956). However, such a shift still only represents a small fraction of that required to account for the interstellar band with a normal nitrile. The exact coincidence of the observed interstellar band with the one appearing on our spectra, points to a molecule containing only H, C, N and probably O. Van de Bult (1986), in his study of the photochemistry of binary mixtures (e.g. $H_2O/CH_4$; $CO/NH_3$; $H_2O/CO$) has shown that the 2167 $cm^{-1}$ band seems correlated with a strong and broad absorption at 1695 $cm^{-1}$. Such an absorption is also clearly visible in our spectra. This band can most probably be attributed to a carbonyl (C≡O) stretching vibration (see e.g. Jones and Sandorfy, 1956, for a review of the position of carbonyl stretching frequencies). Such a functional group attached to the carbon atom next to the cyano group can shift the CN stretching vibration by 35 $cm^{-1}$; for example in pyruvonitrile, $CH_3—\overset{\overset{O}{\|}}{C}—C\equiv N$, the C≡N vibration is at 2230 $cm^{-1}$ and the strong carbonyl absorption is at 1730 $cm^{-1}$ (Pouchert, 1983). Among other possible candidates, cyanogen $C_2N_2$, absorbs strongly at 2166 $cm^{-1}$ (Verderane et al., 1963) making it a plausible carrier of the interstellar band, but since it does not possess any absorption band around 1700 $cm^{-1}$ it cannot account for the laboratory band. Finally, as shown by the quantitative studies described in Sect. 4 the integrated intensities of both the 2167 $cm^{-1}$ and the 1695 $cm^{-1}$ laboratory bands, have to be considerably larger than those of normal nitriles (R—C≡N). Taken together, the above arguments indicate that normal nitriles, such as acetonitrile, are not very attractive candidates for the 2167 $cm^{-1}$ band. Isonitriles R—N≡C, on the other hand, generally absorb at much lower frequencies, in the range 2180–2120 $cm^{-1}$ (Herzberg, 1945; Williams, 1956). Unfortunately, very few infrared spectra of isonitriles have been studied and although the —N≡C band seems to possess the requisite very strong absorption in the 2175–2150 $cm^{-1}$ region, a general statement concerning the absorbance cannot be made (Ugi and Meyer, 1960; Socrates, 1981).

*ii) 1470 $cm^{-1}$ (6.8 $\mu m$).* The appearance of a broad absorption around 1500–1400 $cm^{-1}$ (6.8 $\mu m$) is also quite significant because of the occurrence of a similar broad absorption band in several protostellar objects (Willner et al., 1981). This broad band occurs at the correct frequency for identification with deformation modes in saturated hydrocarbons (Hagen et al., 1980). Unfortunately, the width of this band and the large number of molecules which can account for this absorption makes a precise identification to a specific hydrocarbon impossible. The methyl and methylene deformation modes occur at about the same frequency for various aliphatic hydrocarbons ($CH_3$: 1450 $cm^{-1}$ and 1375 $cm^{-1}$; $CH_2$: 1465 $cm^{-1}$) and, although the relative

strengths of these bands are generally good indicators of the ratio of $CH_2$ to $CH_3$ groups in a given molecule, such an analysis is not possible in these laboratory spectra. However, the shallow absorption bands in the 3.4 $\mu$m region where the CH stretching modes for $CH_3$ and $CH_2$ groups occur, enables us to narrow the range of possible carriers of the 1470 $cm^{-1}$ band (Bellamy, 1956). In general, the absorption strength of the stretching vibrations is considerably decreased ($\div 10$) when a methyl or methylene group is attached to an unsaturated group such as carbonyl (e.g. $CH_3—\underset{|}{C}=O$). The reduction in intensity of this mode is accompanied by a several-fold increase of the intensity of the deformation modes in the 1470 $cm^{-1}$ region (Wexler, 1967; Francis 1951). This is also true, although to a lesser extent, if the methyl group is adjacent to an OH group (Drushel et al., 1963). In our spectra, the presence of a strong band at 1370 $cm^{-1}$ and absence of clear cut absorption at about 2400 $cm^{-1}$ points to the presence of an ester or ketone rather than an alcohol in the mixture. For example the simplest ketone, acetone $(CH_3)_2CO$, absorbs strongly at 1706, 1420, 1367, 1236 and near 1095 $cm^{-1}$ and only weakly to moderately at 3005, 2968 and 2921 $cm^{-1}$ in $H_2O$ (Hagen et al., 1983b). A simple ester, ethylacetate ($CH_3—CO—O—C_2H_5$), also has much weaker bands in the 2900 $cm^{-1}$ region than in the 1000–1700 $cm^{-1}$ region in the solid state (Paper III). A broad band between 1270 and 1220 $cm^{-1}$ is characteristic of the non-carbonyl CO stretch in an ester or the C—C stretch in a ketone (Bellamy, 1956). In the laboratory spectra, the presence of a strong absorption at 6.8 $\mu$m and the almost complete absence of absorption at 3.4 $\mu$m points to the formation of saturated aliphatic hydrocarbons in which the methyl and methylene groups are adjacent to unsaturated groups. Considering the initial ice composition, it is quite likely that these are alkoxy (—O—C=O) and carbonyl (C—(C=O)—)groups. Quite recently, Sandford and Walker (1985) have reported a 6.8 $\mu$m feature in the spectrum of a class of interplanetary particles and assign it to the scissoring vibration of the carbonate group ($CO_3^{--}$). Although this is quite reasonable for the interplanetary particles, it is an unlikely explanation of the 6.8 $\mu$m laboratory band for Mixture 1 because there is not enough oxygen available to produce $CO_3$ in sufficient quantity.

Interestingly enough, there is no evidence for the production of substantial amounts of unsaturated hydrocarbons in these experiments. The CH stretch occurs at frequencies higher than about 3000 $cm^{-1}$ (3.3 $\mu$m), with the aromatic CH stretch (3010 $cm^{-1}$) at the lower limit. For olefins, the generally weak C=C stretching absorptions occur at about 1660 $cm^{-1}$ (6.0 $\mu$m) and are difficult to detect in water rich mixtures where the OH bending mode of water absorbs strongly. This region changes only slightly upon photolysis. The CH bending modes are usually the strongest in alkenes and alkynes and fall between 1000 and 650 $cm^{-1}$ (10 to 15 $\mu$m); little change is found upon photolysis in this region.

#### 4.2.2. Mixture 2 evolution ($H_2O$:CO:$O_2$:$CH_4$:$NH_3$:$N_2$ = 1/1/1/0.3/0.3/0.03)

Although irradiation of mixture 2 shows spectroscopic changes similar to those caused by irradiation of mixture 1, some differences are apparent. First, as is obvious from Fig. 2, the water ice band at 3.08 $\mu$m increases dramatically during photolysis. In the non-photolyzed mixture, isolated water molecules give rise to the bands around 3700 and 3600 $cm^{-1}$ (2.70 and 2.77 $\mu$m). These are due to $H_2O$ multimers (see Allamandola, 1984 and references therein for a discussion of this). The absorption of a UV photon by an $H_2O$ molecule heats the local volume (approximately a sphere several monolayers thick) for a sufficiently long time to allow one or two site diffusion. Eventually this molecule will encounter another diffusing $H_2O$ molecule, forming a rather strong hydrogen bonded dimer, which will grow via the same mechanism (capture of a diffusing $H_2O$ molecule) to a trimer, eventually producing the higher multimers responsible for the position and profile of the 3.1 $\mu$m "ice" band. As the total number of $H_2O$ molecules in the sample does not change appreciably, this process illustrates, particularly effectively, the dramatic increase in the cross section of the OH stretching mode $\nu_3$, by more than a factor of 12 in going from isolated molecules and small multimers to higher multimers of water. During the same irradiation time, however, the absorption band at 6 $\mu$m which is due to the H—O—H bending vibration in the water molecule and the so-called 12 $\mu$m band (librational mode) which occurs at about 14 $\mu$m in these mixtures undergo very little change in intensity upon irradiation showing that the total number of water molecules remains essentially unchanged. Thus, in a mixture where neither the exact amounts of the constituents, the precise conditions and temperature of the ice, nor the quantity of irradiation the ice has received are known, the 3.1 $\mu$m ice band does not reflect the precise quantity of water present in the sample. Naturally this has direct astrophysical implications since, for most objects in which the 3.08 $\mu$m band has been studied, little is known about these conditions. Any quantitative analysis of this band is based on the assumption that all of the $H_2O$ is in a highly multimeric ice form. In this sense, the 6 $\mu$m $H_2O$ band (bending mode) is a far more reliable probe of the amount of water present in mantles. Even though it will most likely be blended with bands due to $NH_3$, $H_2CO$ and XCN, water tends to dominate absorption at this wavelength and possesses a distinct, recognizable profile.

The second major difference in this mixture is the more thorough destruction of the original molecules: methane is more efficiently destroyed and ammonia almost completely disappears after only 4 hr of irradiation. This is presumably due to a combination of the following: in Mixture 1, water, the dominant constituent, could protect these molecules by absorbing the UV photons efficiently, and furthermore, most radicals would be formed adjacent to saturated molecules and reactions would proceed slowly. In Mixture 2 however, $O_2$, which is extremely reactive and easily photolyzed, is abundant and radicals formed adjacent to this molecule will react with it. Consequently, the number of $CO_2$ molecules formed upon photolysis is more abundant in mixture 2 and $CO_2$ production dominates at the expense of CO and naturally $O_2$. $O_2$ photolysis is very efficient with the $H_2$ lamp, producing oxygen atoms with enough excess energy to overcome the small activation barrier for the reaction $CO + O \rightarrow CO_2$, resulting in substantial carbon dioxide formation due to the initial high abundance of carbon monoxide. The photolytic O atoms also react with $O_2$ molecules forming ozone as shown by the strong absorption at 1040 $cm^{-1}$ (9.62 $\mu$m). The much weaker ozone bands at 710 and 2110 $cm^{-1}$ (14.1 and 4.74 $\mu$m), not obvious in Fig. 2, are clearly seen in other experiments. This band is easily confused with the strong methanol ($CH_3OH$) band at 1030 $cm^{-1}$ (9.71 $\mu$m) and discrimination is only possible by comparing these spectra with spectra of ices

containing methanol. Due to the high photodissociation rate of ozone, however, this molecule is never very abundant; it is readily photolyzed back to molecular and atomic oxygen. The net result of this process is to progressively transfer the oxygen into carbon dioxide, ozone being a transition product which diminishes in importance and eventually disappears when the amount of molecular oxygen decreases. Moreover, the high abundance and reactivity of oxygen, either in molecular or atomic form, can be deduced from the observation of three bands which are not present in the spectra of Mixture 1 and which involve molecules containing nitrogen and oxygen atoms. These bands are located at 2235, 1878 and 1615 $cm^{-1}$. The first one can be confidently attributed to the NO stretching vibration in $N_2O$ (Herzberg, 1945; Milligan and Jacox, 1967), which has a very large band strength ($\sim 1.4\,10^3\,cm^{-2}\,atm^{-1}$, Pugh and Rao, 1976), comparable to that of the CO stretch in carbon dioxide ($2\,10^3\,cm^{-2}\,atm^{-1}$, Pugh and Rao, 1976). The other $N_2O$ bands at $\sim 1290$ and 590 $cm^{-1}$ are much weaker and obscured by other absorptions. The 1878 $cm^{-1}$ band is attributed to the NO stretch of NO and the 1615 $cm^{-1}$ band is probably due to the NO stretch in nitrogen peroxide, $NO_2$. This last molecule has a very large band strength for this mode (Herzberg, 1945; $\sim 2\,10^3\,cm^{-2}\,atm^{-1}$, Pugh and Rao, 1976). The other fundamentals of $NO_2$ at $\sim 750$ and 1320 $cm^{-1}$ are much weaker and obscured by other absorptions. Absorption due to the radical HCO is not evident after 4 hours of irradiation and remains weak after 24 hours.

A short summary of the other absorption features which appear upon photolysis is appropriate. A band centered around 6.8 $\mu$m also grows in, more strongly than the corresponding band in Mixture 1. As discussed for Mixture 1, this is presumably due to the deformation modes of aliphatic hydrocarbons. The identification of the 6.8 $\mu$m band in interplanetary particles to the carbonate group ($CO_3^{--}$) by Sandford and Walker raises the question of this band, identified in Mixture 2, where $O_2$ is available. We favor the aliphatic hydrocarbon assignment on the basis of the weak, but correlated bands in the 3.4 $\mu$m region. Note that both the 3.4 and 6.8 $\mu$m bands are more prominent in Mixture 1 than in Mixture 2. $H_2CO$ is also produced as shown here by the weak absorptions at 1720 (shoulder) and 1498 $cm^{-1}$. The absorption at 2167 $cm^{-1}$, observed in Mixture 1 and attributed to the C≡N vibration, and the band at 1695 $cm^{-1}$ believed to be correlated with it, do not appear in this mixture. The presence of the abundant amounts of molecular oxygen, easily photolyzed to hot oxygen atoms, presumably prevents the formation of this CN containing compound, locking up the nitrogen produced from ammonia dissociation in nitrogen oxides ($NO_2$, NO, $N_2O$).

As in Mixture 1, a band at about 1220 $cm^{-1}$ is present in the spectrum. This band is also present in a similar control mixture which does not contain ammonia and hence nitrogen and can be attributed to the C—O—C antisymmetric stretching mode in an ester (Socrates, 1981).

Another interesting weak band grows in at 2043 $cm^{-1}$ which we tentatively attribute to the radical $CO_3$ (not the carbonate ion) for the following reasons: (i) the position is close to the strongest band for this radical (2045 $cm^{-1}$, in a $CO_2$ matrix, Moll et al., 1966), (ii) it disappears upon warmup to 20 K, behavior appropriate to a very reactive species, and (iii) it is formed only in Mixture 2, where there is an adequate source of CO, $CO_2$ and $O_2$ which favors $CO_3$ production via the reactions of the type: $CO^* + O_2 \rightarrow CO_3$ and $CO_2 + O^* \rightarrow CO_3$ (* indicates an excited state species possessing sufficient energy to overcome activation energy barriers). This may have astrophysical significance because a weak absorption at 2040 $cm^{-1}$ has been found in the spectrum of W 33 A (Geballe et al., 1985) which resembles this band. However, the identification of the 2040 $cm^{-1}$ interstellar band with the $CO_3$ radical is uncertain for two reasons. First, the optical depth of this band compared to that of CO in the laboratory spectra is extremely weak; this is not the case in the astronomical spectra, where the ratio of the 2040 of the 2143 $cm^{-1}$ CO band is at least ten times larger. Consequently, such an identification requires that the number of $CO_3$ radicals in the grain mantles with respect to the number of CO molecules towards W 33 A would be too high. Second, experiments in which $H_2S$ was added to similar mixtures and subsequently photolyzed, show the growth of a prominent band at 2040 $cm^{-1}$, presumably due to the CO stretch in OCS, a band which possesses an extremely large cross section ($\sim 3\,10^3\,cm^{-2}\,atm^{-1}$, Pugh and Rao, 1976) and thus should be easily detected even if the cosmic abundance of sulfur is much less than that of O, C and N. These last experiments are reported in Geballe et al. (1985).

### 4.2.3. Difference spectra

To conclude the investigation of the new bands appearing upon photolysis of both mixtures, we display in Fig. 5, the difference spectra from 2000 to 1000 $cm^{-1}$ of these mixtures. These difference spectra are obtained after normalization of the deepest peak, the water bending mode at 1620 $cm^{-1}$. The difference is taken between the spectrum of the non-irradiated and that of

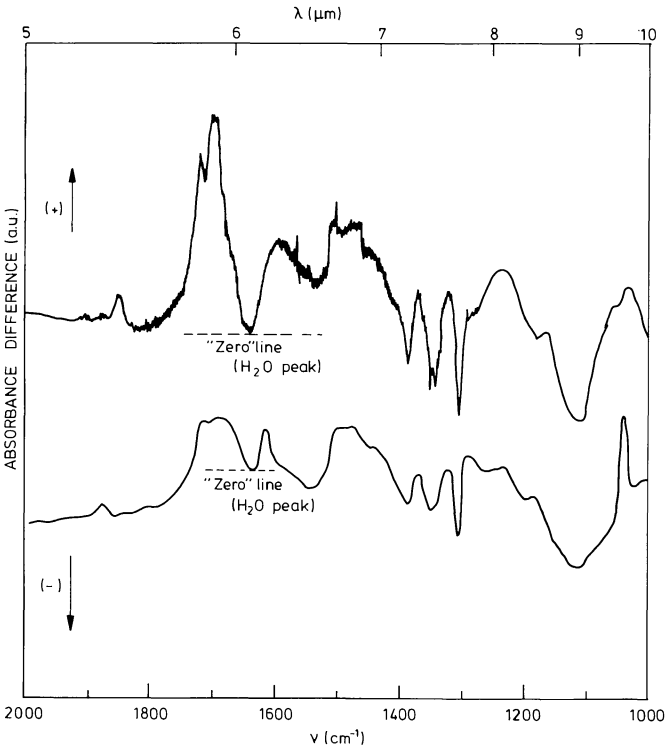


**Fig. 5.** Difference spectra of Mixture 1 (*top*) and Mixture 2 (*bottom*). These are the differences between spectra taken before and after irradiation, normalized to the 6.0 $\mu$m band (see text). In the figure, + and − indicate the direction of band increase or decrease upon irradiation. The zero line is valid for the $H_2O$ 6.0 $\mu$m band

the irradiated mixture. In this figure, bands which grow upon photolysis point upward and those which diminish point downward. Great caution should be taken in the interpretation of these results because the arbitrary normalization at 1620 $cm^{-1}$ is not strictly valid for the whole region considered (2000–1000 $cm^{-1}$) and the intensity ratios of the different lines are not satisfactorily reproduced for lines located under 1400 $cm^{-1}$. This is particularly true for Mixture 2 where the water absorption at 6 $\mu$m is somewhat deeper in the irradiated spectrum than in the original one. Moreover, these difference spectra should not be compared directly with interstellar spectra because this operation tends to artificially enhance weak bands. Nonetheless, when presented this way, spectral features which suffer from some blending are revealed, adding confidence to the analysis.

For Mixture 1 (Fig. 5a), the 1695 $cm^{-1}$ band, is clearly isolated, together with the band at 1720 $cm^{-1}$, attributed to $H_2CO$. The band at 1695 $cm^{-1}$ has a full width at half maximum of about 40 $cm^{-1}$. In Mixture 2 (Fig. 5b), the difference spectrum reveals the presence of a very broad band at about 1685 $cm^{-1}$ (5.9 $\mu$m), having a full width of almost 100 $cm^{-1}$. This band was hidden in the original spectrum (Figs. 2b and c), although the total width of the 6 micron water band could be observed. The $H_2CO$ band at 1720 $cm^{-1}$ is also clearly present in this spectrum as well as the band at 1610 $cm^{-1}$, attributed to $N_2O$. In the two mixtures, the broad band at 6.8 $\mu$m is present, although it is less intense in Mixture 1. Again, in Mixture 1, the difference spectrum reveals the presence of a very broad and shallow absorption band around 1600 $cm^{-1}$, completely absent in Mixture 2. Part of this band could be due to an isocyanide, which has a characteristic absorption around 1590 $cm^{-1}$ and would support the identification of the 2167 $cm^{-1}$ band as being due to a CN group (actually XNC). The band at 1370 $cm^{-1}$ appears in both spectra. In Mixture 2, the band at 1250 $cm^{-1}$ is much less pronounced than in Mixture 1 but this could be due to a problem of normalization.

### *4.3 Residues*

Ices, originally containing simple hydrocarbons (e.g. $CH_4$), photolyzed for a long time and warmed up to room temperature, lead to traces of a non-volatile residue, with an infrared spectrum characteristic of saturated hydrocarbons (Van de Bult, unpublished results, see e.g. Allamandola, 1984). In both Mixtures 1 and 2 however, carbon in the form of methane is not dominant ($\simeq$10%) and consequently a residue rich in saturated hydrocarbons is not expected. During warmup of Mixture 1, after the evaporation of the main volatiles, the 2167 $cm^{-1}$ band carrier remains present on the window up to about 200 K, where it starts to evaporate and has disappeared around 250 K. The band at 1695 $cm^{-1}$, which seems correlated with the 2167 $cm^{-1}$ band, shows the same behavior. After warm-up to about 200 K, all components of the unphotolyzed mixtures have evaporated, revealing the much weaker absorption bands of the residue. Spectra of the less volatile photolysis products from the two mixtures at about 200 K are displayed in Fig. 6. The absorbance scale is expanded by about a factor of 5 the ones used in Figs. 1 and 2. For Mixure 1 (top), three regions of absorption can be noted: a deep broad absorption band centered at about 3000 $cm^{-1}$ (3 $\mu$m), a strong absorption at 2167 $cm^{-1}$ (4.61 $\mu$m) and a broad and deep absorption between 1700 and 1200 $cm^{-1}$ (5.9–8.3 $\mu$m) which shows multiple peaks (1695, 1580, 1460, 1400, 1300 and 1270 $cm^{-1}$). The absorption in the 3000 $cm^{-1}$ region is extremely broad ($\Delta\nu \simeq 600\,cm^{-1}$) and is characteristic of extensive hydrogen bonding of an OH group. The width of this band, and the absorption peak at 2800 $cm^{-1}$, points to the presence of a significant amount of interacting carboxylic acids (Jones and Sandorfy 1962; Bellamy, 1956). Although part of this absorption could be due to some water of hydration in the residue, the absence of the librational mode absorption in the 830–700 $cm^{-1}$ (12–14 $\mu$m) region argues against the presence of much water in this sample. Three peaks are observed at 3200, 3050 and 2820 $cm^{-1}$, the latter could be due to the CH stretch in an aldehyde or in a $CH_3$ group in a compound of the type O—$CH_3$ which, as already mentioned in Sect. 4.2.2, absorbs weakly in this region and more strongly at 1470 $cm^{-1}$. For the other region of the spectrum, the strong absorption at 2167 $cm^{-1}$ is present together with the one at 1695 $cm^{-1}$. During warmup to 200 K, the intensity of the 2167 $cm^{-1}$ band did not change significantly whereas the 1695 $cm^{-1}$ band decreased by a factor of 2–3. Although this result weakens somewhat the hypothesis of correlation between the two bands, selective intrinsic changes in infrared intensities can occur because of changes in the environment of the molecule (not to mention the difficulty associated with the changing baseline at 6 $\mu$m due to the loss of $H_2O$). Additional structure at 1580–1550, 1470, 1400, 1300 and 1270 $cm^{-1}$ are also observed. The first may correspond to an NH deformation band in an alkyl amine (Jones and Sandorfy, 1956), while, as before, the 1470 $cm^{-1}$ band probably corresponds to the $CH_3$ antisymmetric bending mode in hydrocarbons. Finally, the absorptions at 1400 and 1300 $cm^{-1}$ might correspond to a carboxylic acid dimer (Jones and Sandorfy, 1956).

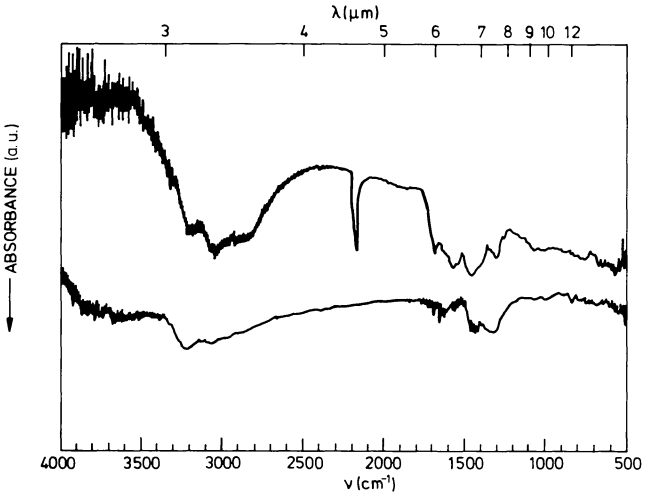


**Fig. 6.** Spectrum of the non-volatile residues remaining on the substrate at 200 K for Mixture 1 (*top*) and Mixture 2 (*bottom*). The abundance scale is expanded by a factor of 5 over that used in Figs. 1 and 2

Mixture 2 has a rather different spectrum at 200 K with the absence of the 2167–1695 $cm^{-1}$ band carrier most striking. Part of the broad feature at 3 $\mu$m remains visible but the peak at 2800 $cm^{-1}$ has completely disappeared. A broad band with two peaks at 1430 and 1310 $cm^{-1}$ is present. Again, the 1430 $cm^{-1}$ band is characteristic of the C—OH stretch in carboxylic acid dimers, this band being accompanied by a band at about 1300 $cm^{-1}$ (Hadzi and Sheppard, 1952).

*4.4 Quantitative estimates*

In this section the number of molecules which grow and/or disappear in the sample during photolysis is estimated. This serves two purposes: firstly, the interpretation of the laboratory experiments requires this analysis to understand the main trends in the formation of new molecular species and, for unidentified molecules, to derive an estimation of the integrated band intensities. This will permit the derivation of a correction to the mantle composition calculated in Paper I. Secondly, since the ultraviolet lamp is calibrated, it is possible to roughly estimate production rates for a few identified molecules, rates which can be compared with those derived in Paper I taking only surface chemistry into account.

It is important to keep in mind that uncertainties exist in the analysis of our experiments. Nevertheless, these data are important because they help to constrain the chemical nature of the unidentified molecules.

4.4.1. Quantitative analysis of the laboratory mixtures

The number of molecules present in the sample is determined using the integrated absorbance values described by d'Hendecourt and Allamandola, (1986). Naturally, such values are valid only for the bands which are not blended with others. For absorptions growing upon photolysis, quantitative estimates can be given with some reliability only when a band assignment to a specific molecule has been made beyond doubt. In Mixture 1 this is true for $CO_2$ and $H_2CO$; in Mixture 2 for $CO_2$, $H_2CO$, $O_3$, NO, $NO_2$ and perhaps $N_2O$. $CO_2$ and $H_2CO$, produced abundantly in both mixtures, will be discussed more extensively.

Table 3 gives the evolution of the number of molecules for both samples before and after 4 and 24 hours of photolysis. Because we are interested in production rates before saturation, the results pertaining to 4 hours irradiation will be discussed in detail. A few general comments are useful: in both mixtures, the original ratio between the molecules is in good agreement with the chosen mixing ratios. The ratio in Mixture 1 is slightly closer than that for Mixture 2, where methane and ammonia are underabundant. In both mixtures, the quantity of water is determined from the absorption in the librational mode around 13 micron. While the number of water molecules seems to remain roughly constant in Mixture 1, the carbon dioxide molecule must be produced by using some oxygen from the water. However this never exceeds 10% of the amount of water an estimate within the level of uncertainty. For Mixture 2, the water content increases. $H_2O$ is made because the photolysis of $CH_4$, $NH_3$ and $O_2$ provides the necessary constituents.

In both mixtures, $CO_2$ is abundantly produced and in Mixture 1, half of the CO which disappears ends up in $CO_2$. For Mixture 2, $CO_2$ is formed much more readily, presumably due to the greater availability of hot atomic oxygen in one photolytic step. For example, one possible reaction set leading to the formation of $CO_2$ in Mixture 1 is

$$H_2O + h\nu \rightarrow H + OH^* \quad (1)$$

$$OH^* + CO \rightarrow CO_2 + H \quad (2)$$

whereas in Mixture 2 we have

$$O_2 + h\nu \rightarrow O + O^* \quad (3)$$

$$CO + O^* \rightarrow CO_2 \quad (4)$$

Because of the concentration of $O_2$ and CO in Mixture 2, $CO_2$ becomes very abundant.

Formaldehyde abundances has been calculated using the difference spectra of the two mixtures and estimating the optical depth of the 1720 $cm^{-1}$ formaldehyde band combined with the band width of 20 $cm^{-1}$ measured by Van der Zwet et al. (1985). $H_2CO$ is more abundant in Mixture 1 than in Mixture 2, again, presumably because the main reaction channel for CO loss is via reaction (4) which can only occur efficiently in Mixture 2. Finally, the abundance of the products NO, $NO_2$, and $N_2O$ in Mixture 2 are estimated. Integrated absorbance values of the gas phase species have been used in calculating these abundances (Gribov and Smirnov, 1962).

The production rate of $CO_2$ and $H_2CO$ in these experiments can be estimated as

$$\alpha = N_m/\Delta t \Phi_{h\nu} \quad (5)$$

where $N_m$ is the number of molecules formed, $\Delta t$ is the irradiation time and $\Phi_{h\nu}$ is the ultraviolet photon flux of the lamp ($\Phi_{h\nu} \sim 10^{15}$ photons $s^{-1}$ $cm^{-2}$). All quantities refer to an area of 1 $cm^2$; roughly the size of the irradiated spot.

We can then derive $\alpha(CO_2) \simeq 4.5\,10^{-3}$ to $1.3\,10^{-2}$ photon$^{-1}$ and $\alpha(H_2CO) \simeq 1.7\,10^{-3}$ to $4\,10^{-4}$ photon$^{-1}$, for Mixtures 1 and 2, respectively. The relevance of these values for the production of these molecules in dense clouds is discussed in Sect. 5.

**Table 3.** The number of molecules ($cm^{-2}$) in both mixtures as a function of ultraviolet photolysis

| | CO | $CH_4$ | $NH_3$ | $H_2O$ | $CO_2$ | $H_2CO$ | $O_3$ | NO | $N_2O$ | $NO_2$ |
|---|---|---|---|---|---|---|---|---|---|---|
| *Mixture 1* | | | | | | | | | | |
| no U.V. | $5.5\,10^{17}$ | $2.1\,10^{17}$ | $2.1\,10^{17}$ | $1.1\,10^{18}$ | — | — | — | — | — | — |
| 4 hrs. | $4.4\,10^{17}$ | $1.7\,10^{17}$ | $1.7\,10^{17}$ | $1.2\,10^{18}$ | $6.5\,10^{16}$ | $2.4\,10^{16}$ | — | — | — | — |
| 24 hrs. | $4.1\,10^{17}$ | $1.3\,10^{17}$ | $6.3\,10^{16}$ | $9.9\,10^{16}$ | $1.4\,10^{17}$ | [a] | — | — | — | — |
| *Mixture 2* | | | | | | | | | | |
| no U.V. | $5.3\,10^{17}$ | $1.2\,10^{17}$ | $9.5\,10^{16}$ | $4.8\,10^{17}$ | — | — | — | — | — | — |
| 4 hrs. | $3.7\,10^{17}$ | $6.0\,10^{16}$ | $1.7\,10^{16}$ | $7.7\,10^{17}$ | $1.9\,10^{17}$ | $5.8\,10^{15}$ | $1.3\,10^{16}$ | $1.5\,10^{16}$ | — | $1.4\,10^{16}$ [b] |
| 24 hrs. | $2.7\,10^{17}$ | $2.6\,10^{16}$ | $1.6\,10^{15}$ | $1.0\,10^{18}$ | $3.7\,10^{17}$ | [a] | $4.5\,10^{15}$ | $2.9\,10^{16}$ | $1.5\,10^{15}$ | [a] |

[a] Not calculated; the poor quality of the spectra in this region after 24 hrs irradiation and the blending with other lines. The 1695 $cm^{-1}$ band and water band prevent this analysis

[b] Magnitude of this band not known. Its value here has been taken equal to the value of the $CO_1$ bending mode at 660 $cm^{-1}$

**Table 4.** Integrated absorbance values A, of a few unidentified bands in Mixture 1, derived using the assumptions described in the text (str ≡ stretch, def ≡ deformation)

| Mode | Band (micron) | Limits ($cm^{-1}$) | $\int I(\nu)d\nu$ | A1 | A2 (cm. molecule$^{-1}$) | A3 |
|---|---|---|---|---|---|---|
| CN-str | 4.62 | 2170–2150 | $7.0\,10^{-1}$ | $1.8\,10^{-17}$ | $2.3\,10^{-17}$ | $3.6\,10^{-17}$ |
| CO-str | 5.88 | 1710–1640 | 1.03 | $4.9\,10^{-17}$ | $4.9\,10^{-17}$ | $4.9\,10^{-17}$ |
| $CH_2/CH_3$ def | 6.80 | 1550–1380 | 1.08 | $2.7\,10^{-17}$ | $1.1\,10^{-16}$ | $5.5\,10^{-17}$ |
| $CH_2/CH_3$ def | 7.30 | 1380–1360 | $1.6\,10^{-1}$ | $4.0\,10^{-17}$ | $1.8\,10^{-17}$ | $9.0\,10^{-18}$ |

4.4.2. Integrated intensities of the 4.62 $\mu$m "CN" and 6.8 $\mu$m "hydrocarbon" bands

The 4.62 $\mu$m band, although assigned to the stretching vibration of the cyano group in a molecule probably containing a carbonyl group (C=O), arises from an unidentified and presumably unique molecule. The 6.8 $\mu$m band, on the other hand, can be assigned to the CH deformation mode in various aliphatic hydrocarbons in the form of alcohols, esters and ketones. This region also corresponds to the deformation mode of the OH group in alcohols. In conjunction with this analysis, two other bands will also be briefly considered here: the first is that near 5.88 $\mu$m (1700 $cm^{-1}$) and the second around 7.3 $\mu$m (1370 $cm^{-1}$). Table 4 lists the strengths for all of these bands, as well as three different estimates for the integrated absorbance values possible. The estimates were made as follows. Except for the 5.88 $\mu$m band, $A_1$ represents the strict lower limit for these cross sections and is obtained by dividing the integrated intensities of each band by the number of carbon atoms available from the photolysis of $CH_4$ (about $4\,10^{16}$ C atoms, see Table 3 for these numbers). For the 5.88 $\mu$m band, presumably due to the carbonyl stretch, the number of carbon atoms is obtained from the difference between the amount of CO lost and the amount of $CO_2$ and $H_2CO$ formed (about $2\,10^{16}$ C atoms). For this band, the number obtained for the infrared cross section shows remarkable agreement with the infrared cross section of the carbonyl group in most molecules ($\approx 10^{-17}$ cm molecule$^{-1}$, Gribov and Smirnov, 1962; Wexler, 1967). The lower limit cross section for the CN band is high, about twice that of the carbon monoxide band $\approx 10^{-17}$ cm molecule$^{-1}$, Person, 1981) and at least ten times that of simple nitriles (Gribov and Smirnov, 1962). The $A_2$ values are derived as follows: assuming a value for the integrated absorbance of the 7.3 $\mu$m of $1.8\,10^{-17}$ cm molecule$^{-1}$, appropriate for $CH_3$ group in acetate, we then calculate the number of $CH_3$ groups in this unknown molecule and assume this number is the same which produces the 6.8 $\mu$m band. This number represents about $1\,10^{16}$ $CH_3$ groups, implying that the cross section of the 6.8 $\mu$m band is remarkably enhanced since the number of C atoms taken from $CH_4$ to form the $CH_3$ is reduced by a factor of 4. The cross section of the CN band is then only slightly enhanced, assuming that the molecule giving rise to the 6.8 and 7.3 $\mu$m bands is not at all related to the one giving rise to the CN band which uses up the rest of C available. Finally, $A_3$ goes one step further in assuming that the unknown molecule containing CN contains all the CO groups responsible for the 5.88 $\mu$m band. As a consequence, the number of carbon atoms available for the 6.8 and 7.3 $\mu$m bands increase by a factor 2 and the values for the cross sections decrease. $A_1$ values are lower limits for these cross sections and their use provides upper limits in the column densities towards interstellar objects where these bands are observed. Column density lower limits can be estimated, within the framework of these assumptions, from the $A_2$ and $A_3$ values with the $A_3$ values preferred. These values should be used with some caution because they are obtained assuming that a given molecule contains only one CN group or one $CH_3$ group.

Although the same analysis could formally be undertaken for Mixture 2, the reaction pathways are different: the carbon dioxide content is very high, slightly higher than the amount of CO available, so that no constraint can be placed in the 1700 $cm^{-1}$ carbonyl band, apart from the fact that its cross section probably has a high value, similar to that obtained in Mixture 1. Moreover, the two carbon reservoirs (CO and $CH_4$) are more intimately mixed because the presence of molecular oxygen promotes the formation of CO molecules from $CH_4$. Because of this uncertainty in CO and $CH_4$ reservoirs, the previous analysis is not repeated. However, we note that the evolution of this mixture in the 6.8 $\mu$m band is similar to that in Mixture 1 and that the cross section of this band is probably large.

4.4.3. Mantle composition after 4 hrs. irradiation

From Table 3, it is possible to derive the new mantle compositions after irradiation. This is given in Table 5 for both mixtures. In Mixture 2, the amount and production rate of $CO_2$ become important. Except for $O_2$ in Mixture 2, note that this table includes only molecules which have been identified in the laboratory spectra. The number of $O_2$ molecules is, a priori, known at $t = 0$ and is estimated, after 4 hours photolysis, by assuming that the total number of oxygen atoms in the samples remains constant. Other more complex molecules are not considered here,

**Table 5.** Corrected mantle composition after 4 hours photolysis (percentage of mantle composition)

| | Mixture 1 | | Mixture 2 | |
|---|---|---|---|---|
| | No UV | 4 hrs. UV | No UV | 4 hrs. UV |
| $H_2O$ | 53 | 58 | 28 | 45 |
| CO | 27 | 21 | 31 | 21 |
| $CH_4$ | 10 | 8 | 7 | 3 |
| $NH_3$ | 10 | 8 | 6 | 1 |
| $O_2$ | — | ? | 29 | 16 |
| $CO_2$ | — | 3 | — | 11 |
| $H_2CO$ | — | 1 | — | 0.4 |
| $O_3$ | — | — | — | 1 |
| NO | — | — | — | 1 |
| $N_2O$ | — | — | — | — |
| $NO_2$ | — | — | — | 1 |

since the amount of complex molecules produced, never exceeds 10% in Mixture 2 and 2% in Mixture 1.

## 5. Astrophysical implications

### 5.1. Gas phase

As described in Paper I, gas and grain chemistry is very different: ion-molecule reactions for the gas phase and low temperature diffusion controlled surface reactions between unsaturated species for the grains. Constant interaction between the two phases is obtained via accretion of the gas phase species onto the grains and molecule ejection from the grains upon explosive reactions between radicals stored within the grain mantle (d'Hendecourt et al., 1982). These radicals are either generated in place by ultraviolet photolysis and cosmic ray bombardment of the icy mantles or accreted directly from the gas and subsequently covered by saturated molecules. The composition of the mantles formed upon accretion and surface reactions has been calculated in Paper I using a relatively simple grain surface chemistry scheme. The influence this interaction with the mantles has on gas phase chemistry was also calculated.

The UV photolysis experiments described in this paper change the composition of the mantles, although it is difficult to quantify the effect this change can have on the gas composition. Carbon dioxide and formaldehyde are produced in significant amounts upon photolysis. Since these two molecules are also present in the gas phase chemistry scheme, they have been chosen to illustrate the role grain mantle photoprocessing has on the production rates of gas phase molecules.

Because accretion and ejection can be considered as two continuous processes, the production rate of a given molecule can be simply written as

$$A = \alpha \Phi_{hv} 4\pi a_d^2 n_d \text{ cm}^{-3}\text{ s}^{-1} \quad (6)$$

where $\alpha$ is the net production rate of the molecule per incident photon, deduced from the laboratory experiments and given in the previous section, $\Phi_{hv}$ is the attenuated ultraviolet flux within the cloud and $4\pi a_d^2 n_d$ is the mean surface area of grains per unit volume in the cloud, $a_d$ and $n_d$ being respectively the radius and number density of the grains. We may tentatively apply this formula for $CO_2$ and $H_2CO$ for which we know the value of $\alpha$. For the standard case as defined in Paper I ($A_v = 4$, $n_0 = 2\,10^4\,\text{cm}^{-3}$), the production rates are $3.8\,10^{-15}$ and $1.4\,10^{-15}\,\text{cm}^{-3}\,\text{s}^{-1}$ for $CO_2$ and $H_2CO$ respectively and calculated with the values obtained from the water rich mixture (Mixture 1). For $CO_2$, this rate is three times less ($\div 3$) than that obtained in the standard model in which the questionable surface reaction $CO + O \rightarrow CO_2$ was allowed. Since this last reaction should not proceed at low temperature (Grim and d'Hendecourt, 1986), the production of carbon dioxide upon mantle photolysis becomes its dominant formation mechanism. For $H_2CO$, the rate obtained here is about one order of magnitude higher than the rate computed in Paper I, at intermediate times ($10^6$ years). The dominant gas phase production mechanism is the neutral-neutral reaction $CH_3 + O \rightarrow H_2CO + H$. The values listed in Table 3 show that ultraviolet photolysis transfers a part of carbon monoxide to $CO_2$ and $H_2CO$. About 12% goes to $CO_2$ and 4% to $H_2CO$ after 4 hrs photolysis of Mixture 1. This represents about $10^7$ years in a cloud where $A_v = 4$. Since CO is an abundant molecule, the production rate of $CO_2$ and $H_2CO$ via this process is quite important.

**Table 6.** Summary of the major bands present in the laboratory spectra including frequencies, wavelengths, bandwidths, behaviour upon photolysis and identifications

| $\nu$ (cm$^{-1}$) | $\lambda$ ($\mu$m) | $\Delta\nu$ (cm$^{-1}$) | $h\nu$ | vib's | Identification |
|---|---|---|---|---|---|
| 3380 (3) | 2.96 | — | d ↘ | N—H str | $NH_3$ |
| 3257 (3) | 3.07 | ~300 | s → | O—H str | $H_2O$ |
| 3010 (4) | 3.32 | ~14 | d ↘ | C—H str | $CH_4$ |
| 2960–2830 | 3.38–3.53 | — | g ↗ | C—H str | X—$CH_3$, X—$CH_2$—Y |
| 2347 (4) | 4.26 | ~20 | g ↗ | CO str | $CO_2$ |
| 2167 (1), (3) | 4.62 | ~30 | g ↗ | CN str | X—N≡C |
| 2143 (3) | 4.67 | ~15 | d ↘ | CO str | CO |
| 1850 (4) | 5.41 | ~18 | g ↗ | CO str | HCO |
| 1720 (2) | 5.81 | — | g ↗ | CO str | $H_2CO$ |
| 1695 (1), (2), (3?), (4) | 5.90 | ~40 | g ↗ | CO str | ? |
| 1640 (3) | 6.1 | ~160 | s → | OH def | $H_2O$ |
| | | | | NH def | $NH_3$ |
| | "6.8" | ~150 | g ↗ | CH def | $XCH_3$, X—$CH_2$—Y |
| 1302 (4) | 7.7 | 9 | d ↘ | CH def | $CH_4$ |
| 1108 | 9.03 | 70 | d ↘ | $NH_3$ umbrella | $NH_3$ |
| 725 (4) | 13.08 | 250 | s → | $H_2O$ hindered rot. | $H_2O$ |
| 660 (4) | 15.02 | 20 | g ↗ | OCO bend | $CO_2$ |

str = stretching vibration; def = deformation mode; bend = bending mode
X, Y = unspecified part of the molecule
(1) = bands correlated
(2) = bands blended with the 1640 cm$^{-1}$ ice band in interstellar souce
(3) = observed interstellar bands
(4) = bands to search for in interstellar spectra (the 1850 cm$^{-1}$ band is rather weak)
$h\nu$ = behaviour upon photolysis ↗ g: growing; → s: steady; ↘ d: decreasing

This shows that, for the production of $CO_2$ and $H_2CO$, photolysis of grain mantles is not only very efficient but is also the dominant mechanism for their formation even if the ultraviolet light is attenuated within the dense clouds. For $CO_2$, a high abundance is expected in the mantle as well as in the gas phase so that, in some cases (Mixture 2 for example), as much as 50% of the available cosmic carbon could well be locked up in $CO_2$. For $H_2CO$, the high production rate deduced here will certainly increase its abundance in the gas, especially in regions of moderate UV extinction ($A_v = 4$ to 6), although it is difficult to predict how much this abundance will be enhanced, due to the complexity of the gas phase scheme, without further calculations.

### 5.2. *Solid phase*

For the solid state features, we limit the discussion to those observed towards W 33 A because this object shows some of the strongest interstellar absorption bands and has a nearly complete spectrum from 3 to 10 $\mu$m. Table 6 summarizes all the major laboratory features. For convenience the spectrum is split into two regions, that around 4.6 $\mu$m and the 5–8 $\mu$m range.

#### 5.2.1. 4.6 micron (2140 $cm^{-1}$) region

This region, observed at low resolution by Soifer et al. (1979), then with higher resolution by Lacy et al. (1984), shows the feature attributed to solid CO and 2140 $cm^{-1}$ as well as the broad and deep feature at 2167 $cm^{-1}$, attributed to the CN stretching vibration. This last feature, undoubtedly present in the photolyzed Mixture 1 spectrum, does not grow upon warmup. Furthermore, the molecule responsible for this absorption evaporates at a temperature above 200 K. The optical depth ($\tau$) of this band in W 33 A has been estimated by Lacy et al. (1984), to be 1.28 with a corresponding full width at half maximum of 27.8 $cm^{-1}$. For CO, these numbers are 0.56 and 12 $cm^{-1}$ respectively. Their derivation for the number of molecules, containing the CN group along the line of sight to W 33 A, was based upon the assumption that the infrared cross section for this band is equal to that of CO corresponding to $\sigma = 1.1\,10^{-17}$ cm molecule$^{-1}$. This implies that the CN group contains about 3.6 times the amount of carbon observed in solid CO. However, as shown in Sect. 4, the lower limit for the cross section of the CN band in the laboratory spectrum is nearly twice as large as that for CO. Thus, assuming the interstellar and laboratory bands have the same carrier, *the upper limit of the column density of the CN containing molecule towards W 33 A is nearly twice the column density of solid CO molecules* in the line of sight.

A feature was recently discovered in the spectrum of W 33 A, located at 2050 $cm^{-1}$. In the laboratory experiments we attribute the weak 2050 $cm^{-1}$ band to $CO_3$. Because the infrared cross section is not known for this molecule, it is impossible to derive the number of molecules present in our samples. As discussed in Sect. 4, although our identification to $CO_3$ is justified in the experiments, sulfur containing molecules show a strong absorption band at this wavelength (Geballe et al., 1985), and further studies are needed to establish a reliable identification of the 2040 $cm^{-1}$ interstellar band.

#### 5.2.2. The 5–8 (2000–1250 $cm^{-1}$) micron region

This spectral region, not accessible from the ground, has been measured from the Kuiper Airborne Observatory by Soifer et al. (1979) for W 33 A. Although the observed absorption band at 6 $\mu$m has been attributed primarily to $H_2O$ (Tielens, 1984), the 6.8 micron band, attributed to scissoring and bending vibrations of $-CH_2-$ and $-CH_3$ groups in aliphatic hydrocarbons (Allamandola, 1984; Tielens et al, 1984), is less well contrained. Figure 7 shows the observed spectrum (dots) together with the spectra of the mixtures water/methanol (3/1), water/ammonia (3/1), and Mixtures 1 and 2 both non-irradiated and irradiated. As is clear from this figure, only the methanol/water mixture and Mixture 1 fall within the error bars of the 6.0 $\mu$m interstellar band with the former somewhat better. Neither of the other mixtures reproduce the width of the 6 $\mu$m band. The 6 $\mu$m band of water appears narrower than the interstellar band in the water ammonia 3/1 mixture and the short wavelength side of the band cannot be matched correctly. This is also true for the spectrum of Mixture 2. The best fit for the 6.0 $\mu$m band is with the $H_2O/CH_3OH$ (3/1) and photolyzed Mixture 1 spectra. The latter is slightly better with the 1720 $cm^{-1}$ band ($H_2CO$) and the broad 1695 $cm^{-1}$ blending with the stronger $H_2O$ band and reproduces quite well the observed shape. We recall here that, in the laboratory spectrum, the 1695 $cm^{-1}$ band seems to be correlated with the 2167 $cm^{-1}$ band and that this last band is observed in W 33 A. Until better signal-to-noise data are available, in which one can draw a reliable short wavelength band edge, it will be difficult to place lower limits on the amount of $H_2CO$ and XCN which can blend with the dominant $H_2O$ 6.0 $\mu$m band.

Absorption in the 6.8 $\mu$m region appears upon photolysis in both Mixtures 1 and 2 and, in terms of peak absorption

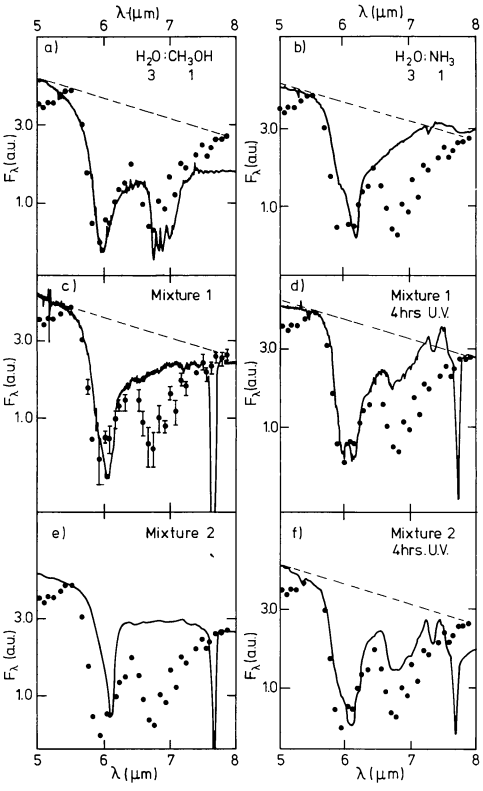


**Fig. 7a–f.** Comparison of the spectrum of W 33 A (dots) and various laboratory mixtures. Intensity units are arbitrary and the spectra are all roughly normalized to the 1620 $cm^{-1}$ (6.0 $\mu$m) water absorption. Observational error bars are shown only in frame (**c**). The spectrum of W 33 A is from Soifer et al. (1979)

and width, the match with the observed spectrum is reasonable. Naturally, the optical density ratio between the 6 and 6.8 $\mu$m bands in the W 33 A spectrum is not reproduced in the laboratory mixtures since this is determined by the relative amounts of species contributing to both bands. It is closer in the water/methanol (3/1) case (Fig. 6a) with the absorption peak due to methanol centered at 6.9 $\mu$m, a slightly longer wavelength compared to what is observed. This shift is not present in the Mixture 1 and 2 spectra. The production of a deeper 6.8 $\mu$m band upon photolysis of Mixture 2 which contains about twice as much methane as Mixture 1 supports the assignment of this band to an aliphatic group. It is reasonable to expect that continual photolysis of both mixtures will yield a deeper 6.8 $\mu$m band until the $CH_4$ is depleted. Note from Figs. 1 and 2 that the integrated band strength of the 6.8 $\mu$m band produced is significantly greater than lost from the $CH_4$ deformation mode at 7.7 $\mu$m. This again points to a relatively large cross section for this 6.8 $\mu$m band. As already postulated in Sect. 4 on quantitative analysis, such large cross sections are expected for aliphatic ketones, esters and alcohols, molecules which are likely to form given the make-up of the initial ices. The short wavelength edge of the 6 $\mu$m absorption band in W 33 A is consistent with the presence of some carbonyl groups in the ices making up the mantles of the grain present along the line of sight.

Finally, we can estimate the amount of molecules responsible for these two bands in the line of sight of W 33 A. The 6 $\mu$m band is largely due to water, although other bands are probably present which extend the short wavelength edge. Following Tielens et al. (1984) we use the peak strength of pure $H_2O$ ($\sim 4.2\,10^{-20}$ cm$^2$ molecule$^{-1}$), measured by Hagen et al. (1981) to estimate the column density. The observed optical depth at the peak maximum is about 2 (Soifer et al., 1979), corresponding to a column density of $4.7\,10^{19}$ cm$^{-2}$ (see Tielens et al., 1984 for a thorough discussion of this). For the 6.8 $\mu$m band, we use the experimental $A$ values derived in Sect. 4 (Table 6) to estimate an upper limit of $8.8\,10^{18}$ cm$^{-2}$, corresponding to $A_1$, and lower limits between $2.2\,10^{18}$ and $4.3\,10^{18}$ cm$^{-2}$, based on the assumptions made in Sect. 4.

Thus, if we identify the 6.8 $\mu$m band in W 33 A with aliphatic hydrocarbons, all of which are adjacent to unsaturated groups such as C=O, the column density of C in these molecules represents at best 11% of all the carbon present in this line of sight with absolute lower limits between about 3 and 6.5%. This number is based on the total carbon reservoir as estimated in Tielens et al. (1984) by taking into account the optical depth in the silicate band (Willner et al., 1982) and deriving a total hydrogen column density with the standard assumptions ($A_v/\tau_{9\,\mu m} = 15$, Gillett et al., 1975 and $N_H/A_v = 1.9\,10^{21}$ cm$^{-2}$, Bohlin et al., 1978). Based on the assumption that the 6.8 $\mu$m band arises from aliphatic groups in saturated hydrocarbons (i.e., not adjacent to unsaturated groups), Tielens et al. (1984) show that about 30% of all the carbon along the line of sight toward W 33 A is required to account for the optical depth. In general, integrated absorbance values of aliphatic hydrocarbons will fall within the range of those used to derive the estimates of 30% and 11% (or 6.5 and 3%).

The recent, alternate suggestion by Sandford and Walker (1985) that the 6.8 $\mu$m band in W 33 A and other interstellar objects could be due to the carbonate ion rather than aliphatic hydrocarbons can only be resolved by better spectroscopic observations of the interstellar objects, looking for correlations with the other bands expected. For example, the difficulty in measuring interstellar bands at 3.4 $\mu$m points to hydrocarbons in which the aliphatic groups are adjacent to electro-negative groups. Certainly, the composition of interstellar ices and structure in the 6.8 $\mu$m band is consistent with this (Tielens et al., 1984). The carbonate identification implies the presence of weaker bands at about 9.3, 11.5 and 14 $\mu$m, also difficult spectroscopic regions to search.

## 6. Conclusions

A semi-empirical method for the treatment of chemical reactions within molecular mantles accreted on interstellar grains is used to probe grain mantle evolution in dense molecular clouds. The compositions of the mantle analogs used in the laboratory have been chosen on the basis of a model which takes into account gas phase and solid state reactions.

Energetic processes such as UV photolysis described here, bring modifications to the mantle and influence the gas phase chemistry and composition. It has been shown that carbon dioxide and, to a lesser extent, formaldehyde are made abundantly upon photolysis in the mantle. This process constitutes a dominant formation mechanism for these two molecules and can contribute significantly to the gas phase abundance.

In addition, upon photolysis, new bands appear in the infrared spectrum of the two samples at 4.62 and 6.8 $\mu$m which have been observed in the spectra of interstellar objects.

Comparison of the spectrum of the protostellar object W 33 A with that of the photolyzed laboratory mixtures, points to be presence of molecules containing aliphatic groups which are adjacent to unsaturated groups as in ketones, esters and alcohols. In these types of molecules, the 6.8 $\mu$m absorption features can be enhanced by as much as a factor of 10 with respect to that at 3.4 $\mu$m. The absence of a prominent 3.4 $\mu$m band, superimposed on the wing of the ice band in interstellar objects showing a strong 6.8 $\mu$m feature, suggests the presence of these types of molecules in space.

The observed, relatively deep features at 4.62 and 6.8 $\mu$m in W 33 A, compared to the laboratory simulations show that the grain mantles are indeed highly processed. While these bands could be carried by molecules produced in low energy cosmic-ray induced reactions which show similarities with the processes reported here (Moore, 1981; Moore and Donn, 1982), the depths of the bands imply a degree of processing inconsistent with current estimates of cosmic ray flux, implying that it is primarily due to UV which is present in the cloud. This cosmic-ray processing however, could be more efficient than photolysis in denser regions where the ultraviolet light does not penetrate. Here, its effectiveness is increased by the fact that cosmic rays have a high penetrating power and are able to ionize the mantle material (Brown et al., 1978) and hence increase the efficiency of the process.

The absence of prominent features at 3.4 $\mu$m in the laboratory spectra while they are indeed observed in the diffuse clouds towards the galactic center (Allen and Wickramasinghe, 1981) might be due to the fact that diffuse cloud grains are more photoprocessed than those imbedded in dense molecular clouds. The galactic center spectra also lack an ice band and so blending is minimal. Furthermore, highly photoprocessed materials tend to gradually lose oxygen and saturated hydrocarbons and highly polymeric residues can be expected (Van de Bult, unpublished results, Schutte et al., 1985).

This work represents the first order attempt to address several questions related to interstellar chemistry, grain mantle composition, photoprocessing, and infrared observations. As such, only some areas have been touched upon and much work remains to be done to test some of the assumptions and explore the various hypothesis. For the short term, future experiments in the laboratory should concentrate on making a more precise identification of the molecules responsible for the new absorptions. This is particularly true for the XCN band carrier, which should be studied carefully in order to measure its precise cross section in the infrared. Quantitative evaluation of the same effects produced by low energy cosmic ray irradiation will also be useful. For the longer term, far infrared experiments should be undertaken to study the properties of these mixtures, non-irradiated as well as irradiated. The 20–30 $\mu$m region will show deformation modes of many carbon bearing molecules, for example, the nitriles have a very strong absorption around 27 $\mu$m. At longer wavelength, the lattice modes of these molecular solids are completely unknown and will provide considerable information about the structure of these mixtures, particularly their degree of mixing and crystallinity. The laboratory study of the 45 $\mu$m band of water, pure and in a mixture, will be of particular importance to understand the physical and chemical nature of the water rich ices.

Finally, it is worthwhile reviewing what the most important regions of the infrared spectrum are from a grain composition point of view. From 2.6 to 3.1 $\mu$m, isolated molecules of water possess identifiable bands, very useful to study the degree of mixing and the proportions of water in a given spectrum. Overtone bands of carbon dioxide are also present in this region. At 4.27 $\mu$m, carbon dioxide should easily be detected not only because of its abundance but also because of its unusually large cross section. The 5 to 8 $\mu$m region, although very promising for the detection of HCO (5.4 $\mu$m), water and some "hydrocarbons" will be more difficult to interpret because of line blending with bands from different molecules. High resolution data with a good signal-to-noise ratio will be needed in order to detect $CH_4$ at 7.7 $\mu$m as well as separate the other bands. Finally, the librational mode of water, located at 13.2 $\mu$m, a very broad and probably shallow band (FWHM $\sim$4.2 $\mu$m) should be detectable in objects where the 3 $\mu$m ice band is observed to be strong. In the wing of this band, the absorption of $CO_2$ at 15.2 $\mu$m should be present, although it is about ten times weaker than the 4.27 $\mu$m band.

*Acknowledgements.* We thank G. van der Zwet for permission to use his spectrum of formaldehyde (Fig. 4). Many discussions about the identification of the lines observed in the laboratory spectra and the relevance of this work to the interpretation of astronomical spectra have improved the quality of this work. For these discussions, we thank particularly F. Baas, C.E.P.M. van de Bult, L.J. van IJzendoorn and G. van der Zwet in Leiden and A.G.G.M. Tielens at NASA, Ames.

## References

Aitken, D.K.: 1981, in *Infrared Astronomy*, IAU Symposium, No. 96, eds. G.G. Wynn-Williams, and D.P. Cruishank, D. Reidel Publishing Co., Dordrecht, p. 207.

Allen, D.A. Wickramasinghe, D.T.: 1981, *Nature* **294**, 239

Allamandola, L.J.: 1984, in *Galactic and Extragalactic Infrared Spectroscopy*, eds. M.F. Kessler, J.P. Phillips, D. Reidel Publishing Co., Dordrecht, p. 5

Bellamy, L.J.: 1956, in *The Infrared Spectra of Complex Molecules*, John Wiley and Sons, Inc., New York

Bohlin, R.C., Savage, B.D., Drake, J.F.: 1978, *Astrophys. J.* **824**, 132

Dressler, K., Schnepp, O.: 1960, *J. Chem. Phys.* **33**, 270

Drushel, H.V., Senn, Jr., W.L., Ellerbe, J.S.: 1963, *Spectro-chim. Acta* **19**, 1815

Francis, S.A.: 1951, *J. Chem. Phys.* **19**, 942

Geballe, T.R., Baas, F., Greenberg, J.M., Schutte, W.: 1985, Astron. Astrophys. **146**, L6

Gillett, F.C., Jones, T.W., Merrill, K.M., Stein, W.A.: 1975, *Astron. Astrophys.* **45**, 77

Graedel, T.E., Langer, W.D., Frerking, M.A.: 1982, *Astrophys. J. Suppl.* **48**, 321

Gribov, L.A. Smirnov, V.N.: 1962, *Soviet Physics Uspekhi* **4**, 919

Greenberg, J.M.: 1982, in *Comets*, L.L. Wilkening, ed., University of Arizona Press, p. 131

Grim, R., d'Hendecourt, L.B.: 1986, *Astron. Astrophys.* (submitted, Paper IV)

Hack, W., Langel, W.: 1981, *Chem. Phys. Letters* **81**, 387

Hadzi, D., Sheppard, N.: 1952, *Proc. Roy. Soc.* **A216**, 274

Hagen, W., Allamandola, L.J., Greenberg, J.M.: 1979, *Astrophys. Space Sci.* **65**, 215

Hagen, W., Allamandola, L.J., Greenberg, J.M.: 1980, *Astron. Astrophys.* **86**, L3

Hagen, W., Tielens, A.G.G.M., Greenberg, J.M.: 1981, *Chemical Phys.* **56**, 367

Hagen, W., Tielens, A.G.G.M., Greenberg, J.M.: 1983a, *Astron. Astrophys.* **117**, 132

Hagen, W., Tielens, A.G.G.M., Greenberg, J.M.: 1983b, *Astron. Astrophys. Suppl.* **51**, 389

d'Hendecourt, L.B.: 1984, Ph.D. Thesis, University of Leiden, The Netherlands

d'Hendecourt, L.B., Allamandola, L.J., Baas, F., Greenberg, J.M.: 1982, *Astron. Astrophys.* **109**, L12

d'Hendecourt, L.B., Allamandola, L.J., Greenberg, J.M.: 1985, *Astron. Astrophys.* **152**, 130 (Paper I)

d'Hendecourt, L.B., Allamandola, L.J.: 1986, *Astron. Astrophys. Suppl.* (in press, Paper III)

Hemert, M.C. van: 1981, Ph.D. Thesis, University of Leiden, The Netherlands.

Herzberg. G.: 1945, in Molecular Spectra and Molecular Structure II, Infrared and Raman Spectra of Polyatomic Molecules, Van Nostrand, Princeton, New Jersey

Jones, N.R., Sandorfy, C.: 1956, in *Chemical Applications of Spectroscopy*, Vol. 9, Interscience Publishers, Inc. New York, p. 247

Kitson, R.E., Griffith, N.E.: 1952, Analytical Chem. **24**, 234

Knacke, R.F., McCorkle, S., Puetter, R.C., Erickson, E.F., Krätschmer, W.: 1982, *Astrophys. J.* **260**, 141

Lacy, J.H., Baas, F., Allamandola, L.J., Persoon, S.E., McGregor, P.J. Lonsdale, C.J., Geballe, T.R., van de Bult, C.E.P.: 1984, *Astrophys. J.* **276**, 533

Leger, A., Klein J., de Cheveigne, S., Guinet, C., Defourneau, D., Belin, M.: 1979, *Astron. Astrophys.* **79**, 256

Milligan, D.E., Jacox, M.E.: 1964, *J. Chem. Phys.* **41**, 3032

Milligan, D.E., Jacox, M.E.: 1967, *J. Chem. Phys.* **47**, 5146

Milligan, D.E., Jacox, M.E.: 1971, *J. Chem. Phys.* **54**, 927

Moll, N.B., Ckitter, D.R., Thompson, W.E.: 1966, *J. Chem. Phys.* **45**, 4469

Moore, M.H.: 1982, Ph.D. Thesis, University of Maryland, USA

Moore, M.H., Donn, B.: 1982, *Astrophys. J.* **257**, L47
Morton, D.C.: 1974, *Astrophys. J.* **143**, L35
Okabe, H.: 1978, in Photochemistry of Small Molecules, John Wiley and Sons, New York
Person, W.B.: 1981, in Matrix Isolation Spectroscopy, A.J. Barnes et al., eds., D. Reidel Publishing Company, p. 415
Pouchert, C.J.: 1983, in The Aldrich Library of Infrared Spectra, Aldricht Chemical Company, Milwaukee, Wisconsin
Prasad, S.S., Huntress, W.T.: 1980, *Astrophys. J. Suppl.* **43**, 1
Pugh, L.A., Rao, K.N.: 1976, in *Molecular Spectroscopy: Modern Research*, Vol. II, K.N. Rao, ed., Academic Press, New York, p. 165
Sandford, S.A., Walker, R.M., 1985, *Astrophys. J.* (in press)
Schutte, W., Greenberg, J.M., Ferris, J.P., Agarwal, V.K., Briggs, R., Connor, S., van de Bult, C.E.P.M., Baas, F.: 1985, Origin of Life (in press)
Shimanouchi, T.: 1972, in Tables of Molecular Frequencies Consolidated Volume **1**, NSRDS-NBS No. 39
Socrates, G.: 1981, in Infrared Characteristic Group Frequencies, John Wiley and Sons, New York
Soifer, B.T., Puetter, R.C., Russell, R.W., Willner, S.P., Harvey, P.H., Gillett, F.C.: 1979, *Astrophys. J.* **232**, L53
Tielens, A.G.G.M.: 1984 in *Laboratory and Observational Infrared Spectra of Interstellar Dust*, Hawaii Workshop, July 1983, R.D. Wolstencroft, J.M. Greenberg, eds. Occasional Reports of the Royal Observatory Edinburgh No. **12**, 41
Tielens, A.G.G.M., Hagen, W.: 1982, *Astron. Astrophys.* **114**, 245
Tielens, A.G.G.M., Allamandola, L.J., Bregman, J., Goebel, J., d'Hendecourt, L.B., Witteborn, F.C.: 1984, *Astrophys. J.* **287**, 697
Ugi, I., Meyer, R.: 1960, *Chemische Berichte* **93**, 230
Van de Bult, C.E.P.M.: 1986, Ph.D. Research, University of Leiden, The Netherlands
Van Thiel, M., Becker, E.D., Pimentel, C.C.: 1957, *J. Chem. Phys.* **59**, 5199
Van der Zwet, G.P., Allamandola, L.J., Baas, F., Greenberg, J.M.: 1985, *Astron. Astrophys.* **145**, 262
Verderane, F.D., Nebgen, J.W., Nixon, E.R.: 1963, *J. Chem. Phys.* **39**, 2274
Wexler, A.S.: 1967, *Applied Spectrosc. Rev.* **1**, 29
Whittet, D.C.B., Bode, M.F., Longmore, A.J., Baines, D.W.T., Evans, A.: 1983, *Nature* **303**, 218
Williams, R.L.: 1956, *J. Chem. Phys.* **25**, 656
Willner, S.P., Gillet, F.C., Herter, T.L., Jones, B., Krassner, J., Merrill, K.M., Pipher, J.L., Puetter, R.C., Rudy, R.J., Russell, R.W., Soifer, B.T.: 1982, *Astrophys. J.* **253**, 174